

# Optical and Structural Studies of Silver Oxide Thin Films

Karamvir Tanwar and David Joseph

Department of Physics, Guru Jambheshwar University of Science & Technology, Hisar (Haryana) India -125001

Received: 26 Oct. 2024, Revised: 9 Dec. 2024, Accepted: 21 Dec. 2024

Published online: 1 Jan. 2025

**Abstract:** In this study, silver oxide thin films were deposited at room temperature using thermal evaporation on glass substrates. The films' structural, surface morphological, and linear optical properties were analyzed. X-ray diffraction (XRD) analysis indicated that the films exhibit a cubic structure. Field emission scanning electron microscopy (FE-SEM) revealed an average grains size between 38 nm and 43 nm. Energy dispersive X-ray spectroscopy (EDX) confirmed the presence of silver (Ag) and oxygen (O) in the samples. UV-Vis, FTIR, and laser Raman spectroscopy were also conducted on thin films.

**Keywords:** Thermal Evaporation, FESEM-EDS, Raman spectra, XPS, UV Analysis.

## 1. Introduction

Silver oxide can be found in multiple oxidation states including  $\text{Ag}_2\text{O}$ ,  $\text{AgO}$ ,  $\text{Ag}_3\text{O}_4$ , and  $\text{Ag}_2\text{O}_3$ . Among various forms, the most thermodynamically stable is  $\text{Ag}_2\text{O}$ , which can exist at high partial pressures of oxygen and low temperatures [1, 2]. Research has explored the potential applications of silver oxide thin films across a range of fields, such as photovoltaics, high-density optical devices, optical memories, organic light-emitting diodes, plasmonic photonic devices, and precursor materials for high-temperature superconductors. Similarly, as an antibacterial coating, silver oxide is also utilized in contemporary medicine [3]. The diverse crystal structures of silver oxides lead to a variety of intriguing physical and chemical properties, including those relevant to optics, electronics, photonics, and non-linear optical systems. Owing to the varieties of applications, silver oxide gained special attention regarding the synthesis of nanoparticles and the formation of thin films which further offer a higher surface area to volume ratio and quantum confinement effect leading to the use of silver oxide in nanotechnology [4].

The process used to grow these thin films, along with innovative experimental setups, significantly influences their characteristics, resulting in a broad spectrum of properties even for a single material. Notably, silver oxide thin films exhibit considerable variation, particularly in their electrical and optical characteristics [5]. Using pure oxide as the starting material is preferable for depositing metal oxide thin films. The main techniques for depositing  $\text{Ag}_2\text{O}$  films are electron-beam evaporation and reactive sputtering of silver metal in an argon environment enriched with oxygen. The pulsed laser deposition technique is an additional technique. Nevertheless, the best and the cost-effective other technique is thermal deposition for the synthesis of silver oxide thin films. The thermal evaporation process is commonly utilized in laboratories and industries due to its

precision, allowing for easy control over preparative conditions such as evaporation rate, film thickness, surface morphology, and structural characteristics. These techniques work in the gaseous phase, therefore vacuum conditions and high temperatures were found to be necessary parameters [6]. The properties like porosity and crystallinity depend highly on the reactive oxygen environment during deposition in the case of Sputtering as compared to thermal deposition. Previous research by Fortiu and Weichman [7] has indicated that silver oxide exhibits p-type semiconductor characteristics with a band gap of approximately 1.2 eV, while other studies have reported a wider range of band gaps between 1.2 and 3.4 eV. This indicates that the diverse crystalline phases and properties of thin films, which arise from different deposition techniques, contribute to the wide range of band gaps [8, 9]. Additionally, the substrates compatible with these high-temperature methods are limited to those that can withstand high temperatures, such as quartz, glass, and silicon [10, 11].

The goal of this work was to examine the characteristics of the films made from the thermal evaporation of pure  $\text{Ag}_2\text{O}$  powder using structural and optical studies. Here, we have deposited  $\text{Ag}_2\text{O}$  this film on a glass substrate using the thermal evaporation technique. The prepared thin films have been subjected to various analytic techniques such as X-ray diffraction, FE-SEM, EDS, XPS, UV-visible spectroscopy, FTIR, and Laser Raman Spectroscopy for their structural, morphological and optical properties. One of the special properties of silver oxide that led to its promising technological applications is its thermal breakdown into oxygen and silver. Silver oxide has a reflectivity of over 70% across a very broad wavelength range. The material can be used to replace the widely used organic storage material in short-wavelength optical data storage, which is an advantage. Researchers were drawn to the silver-oxygen system (Ag-O) because of its innovative uses in blue optical lasers, anti-reflective coating and optoelectrical field.

\*Corresponding author E-mail: [davidjp707@gmail.com](mailto:davidjp707@gmail.com)

## 2. Experimental Procedure

Silver oxide thin films were prepared at room temperature using the thermal evaporation coating technique. The starting material was black  $\text{Ag}_2\text{O}$  powder (Alfa Aesar, 99.9% purity) with a melting point of  $300^\circ\text{C}$ , which served as the target material in a molybdenum boat. This material was gradually outgassed before the evaporation process. The films were deposited onto unheated glass substrates, with the resulting thickness measured at approximately 140 nm. The glass substrates were cleaned with acetone using an ultrasonic method, followed by rinsing with distilled water and air drying. The distance between the molybdenum boat and the substrate was set at 8 cm. The entire procedure was conducted in a vacuum chamber with a pressure of around  $5 \times 10^{-4}$  mbar. Following the synthesis, optical and structural characterizations of the deposited films were performed using Laser Raman Spectroscopy and X-ray diffraction (Rigaku, Smart Lab 3KW). Surface morphology and elemental composition analyses were carried out using FESEM-EDS (7610 F Plus/JEOL). Figure 1 displays typical images of the deposited silver oxide thin films on glass substrates.

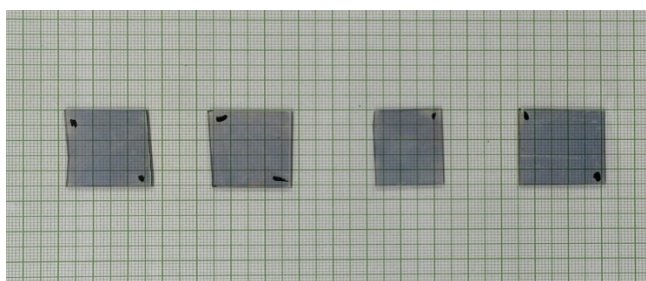


Fig. 1: Deposited  $\text{Ag}_2\text{O}$  thin film on glass substrates

## 3. Materials and methods

### 3.1 X-Ray Diffraction (XRD)

X-ray diffraction with  $\text{Cu-K}\alpha$  radiation ( $\lambda = 0.154056$  nm) was utilized to examine the crystalline phases of the prepared films over a  $2\theta$  range of  $20^\circ$  to  $80^\circ$ . Figure 2 displays the X-ray diffraction pattern of the as-deposited  $\text{Ag}_2\text{O}$  film. The pattern reveals two weak diffraction peaks at (220) and (311), alongside a strong and sharp peak at (111) for  $\text{Ag}_2\text{O}$ . This indicates that the  $\text{Ag}_2\text{O}$  film is oriented, and the XRD pattern confirms its cubic crystalline structure [12].

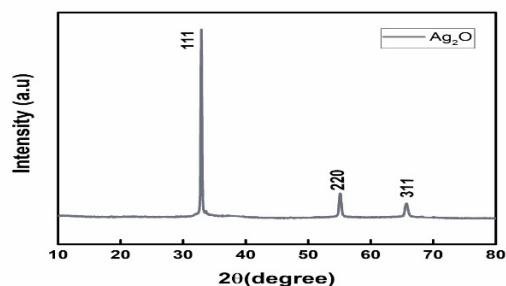


Fig. 2: XRD Pattern of the  $\text{Ag}_2\text{O}$  thin film

### 3.2 Laser Raman Spectra

Raman spectra of the  $\text{Ag}_2\text{O}$  film were obtained at 532 nm excitation using Laser Raman Spectroscopy (Witec UHTS Model 300). Several peaks were identified and compared to standard Raman data for  $\text{Ag}_2\text{O}$  thin films, as shown in Figure 3. The measurements were conducted over a wavelength range of 200–500 nm. The presence of Raman-active modes helps assess the degree of short-range structural order. The modes observed at 230, 249, 317, 435, and  $475\text{ cm}^{-1}$  are associated with the internal vibrations of silver oxide. These peaks in the Raman spectra correlate well with previously reported findings [13,14].

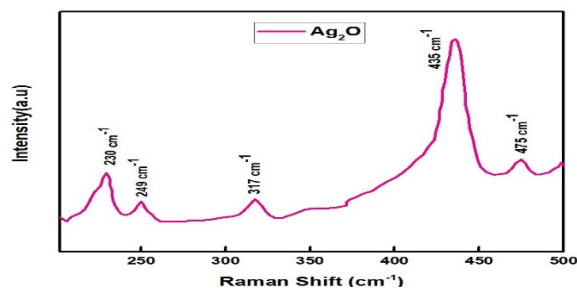


Fig. 3: Raman spectra of silver oxide thin film

Table 1: shows the comparison between the reported literature and our data

Sr. No.	Raju N.R.C et al. [13]	Tsenzughul et al. [14]	Our Data
1.	216	219	---
2.	300	237	230
3.	379	305	249
4.	429	332	317
5.	467	470	435
6.	487	487	475

### 3.3 FE-SEM Studies

FESEM images with different magnifications have been recorded using FESEM-EDS (7610 F Plus/JEOL). SEM images of deposited silver oxide thin film, 25000x magnification 4(b), 50000x magnification 4(c), 100000x magnification 4(d) with average grain sizes (increasing from 38 nm to 43 nm) and 100000x magnification 4(e) with average porosity (increasing from 28 nm to 31 nm) of the deposited thin films sample are recorded. Spherical shapes (like Nanoglobular agglomeration) morphology of silver oxide nanoparticles has been observed in FESEM studies [15].

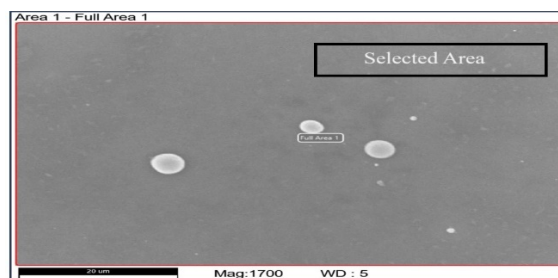
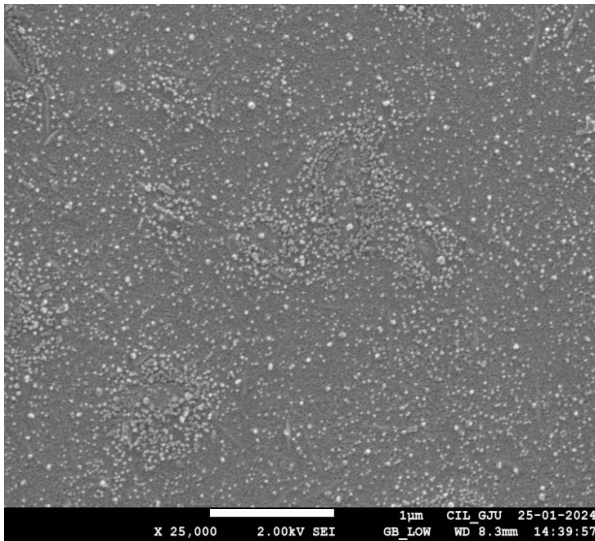
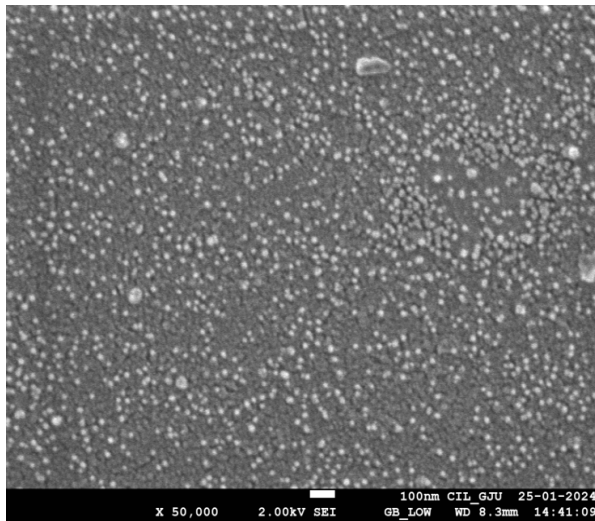


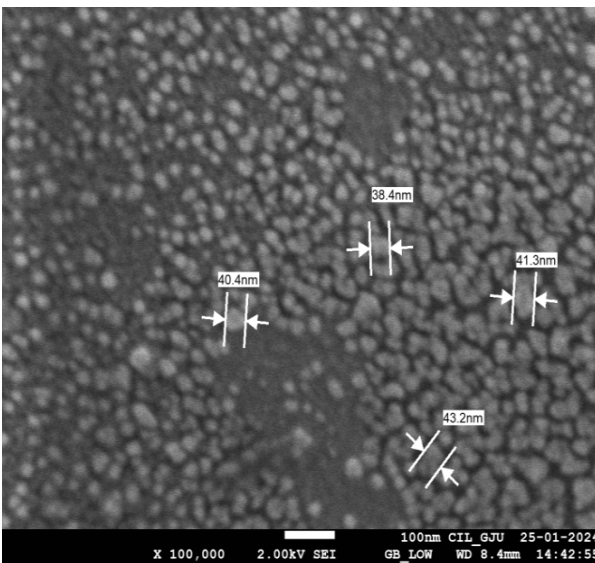
Fig. 4(a): Shows the selected area for magnifications for the silver oxide thin film.



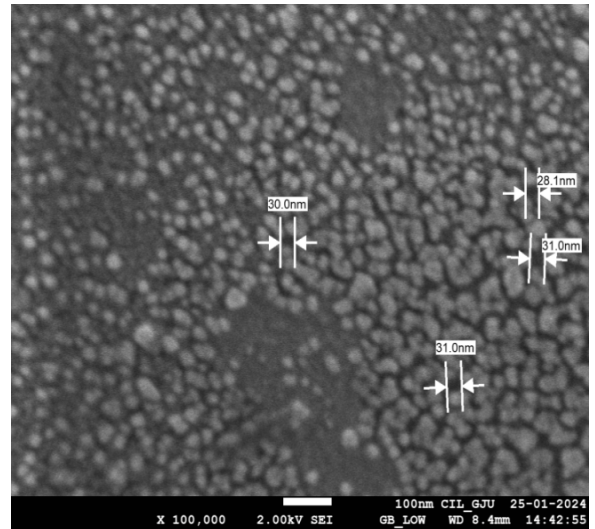
4(b). 25000x



4(c). 50000x



4(d). Grain sizes  $38 \pm 5$  nm



4(e). Porosity  $28 \pm 3$  nm

### 3.4 EDX Analysis

The EDX spectra have been recorded using the FESEM-EDS (7610 F Plus/JEOL) system to provide additional proof and to verify the elemental composition and purity of the synthesized  $\text{Ag}_2\text{O}$  thin films. Fig. 5 shows the typical EDX spectrum of  $\text{Ag}_2\text{O}$  thin film. EDX analysis confirms that Silver and Oxygen are the only elements involved in the synthesis of thin films [16].

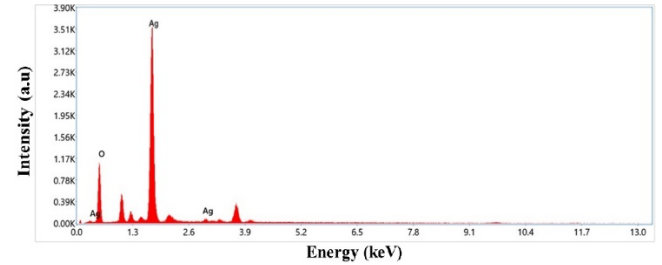


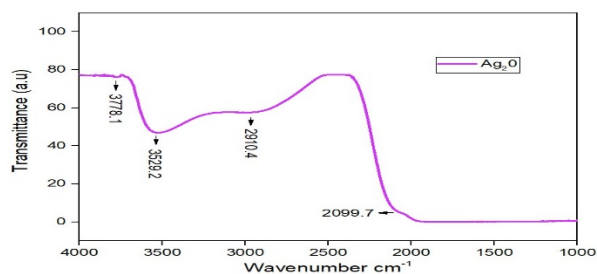
Fig. 5: Shows the prominent peaks for Silver and Oxide

Table 2: Elemental composition of silver and oxide

Sr. No.	Element	Expected Atomic %	Observed Atomic %
1.	O	33.3	27.3
2.	Ag	66.6	73.6

### 3.5 Fourier Transform Infrared Spectroscopy (FTIR)

The Fourier transform infrared spectroscopy (FTIR), model Perkin Elmer operates in the frequency range of  $4000-1000 \text{ cm}^{-1}$ . We obtained every peak in the functional group (diagnostic area) between  $4000$  and  $1500 \text{ cm}^{-1}$ . Peaks  $2099.7 \text{ cm}^{-1}$ ,  $2910.4 \text{ cm}^{-1}$ , and  $3778.1 \text{ cm}^{-1}$  were short and had weak signals, whereas peak  $3529.2 \text{ cm}^{-1}$  had a large signal. These peaks in the FTIR plot were caused by weak interactions between functional groups. The Ag-O-Ag bonding and the O-H stretching vibration modes are responsible for the FTIR peaks, which are consistent with the silver oxide FTIR spectra published in earlier works [17, 18]. Fig. 6 below provides a graphical depiction of FTIR spectral data for silver oxide thin films.



**Fig. 6:** FTIR spectra of silver oxide thin film

**Table 3:** Shows the FTIR data for silver oxide thin film

List No.	Ag <sub>2</sub> O cm <sup>-1</sup> (X)	T % (Y)
1	2099.7	8
2	2910.4	62
3	3529.2	50
4	3778.1	80

### 3.6 UV-Visible spectroscopy

UV-visible absorption spectroscopy was used to study the optical absorption of silver oxide thin films. The outer electrons of atoms or molecules in the UV-visible spectrum are absorbed by radiant energy and change into higher energy states. The energy band gap of the silver oxides in this phenomenon can be obtained by analyzing the spectrum resulting from optical absorption. Since the shift of electrons in the  $\sigma$  and  $\pi$  orbitals from the ground state to higher states occurs during the absorption of UV and visible light, the spectrum provides information about the structure of the molecule. This optical absorption coefficient was computed between 200 and 800 nm in wavelength. A shorter wavelength was used to obtain the absorption edge. The nanoparticles absorption edge measures at 380 nm. As a result, a significant violet shift was obtained at the absorption edge. Over the whole visible spectrum, the silver oxide nanoparticles have outstanding transmission. The transparency lower cut-off (200 nm- 400 nm) and optical transmittance window are mainly used in optical applications, which is why the lower cut-off wavelength is 380 nm. For materials used in optoelectronic device applications, transparency in the visible spectrum is a desired characteristic. It shows that the near-IR, visible, and UV regions of the silver oxide thin film reveal good transparency, suggesting that it can find application in devices [19].

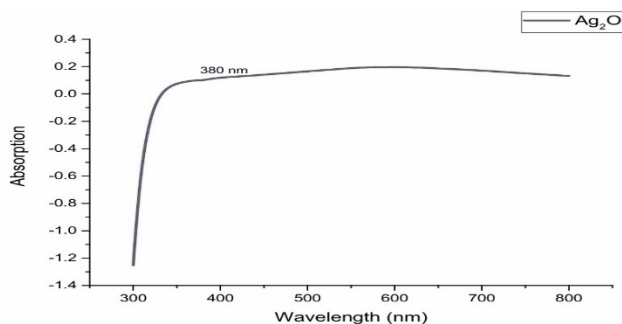


**Fig. 7:** Shows the optical absorption spectrum of silver oxide thin films

### 3.7 X-ray photoelectron spectroscopy (XPS)

The X-ray photoelectron spectroscopic studies were performed on the Ag<sub>2</sub>O films formed on the glass substrate in order to determine the shift of core-level binding energies present in the sample. The binding energy range of 360 eV to 380 eV is where the Si3d core level spectra are recorded [20]. Figure 7 shows the Ag 3d<sub>5/2</sub> and 3d<sub>3/2</sub> peaks for the sample grown where Ag 3d<sub>5/2</sub> peak at 373.8 and Ag 3d<sub>3/2</sub> at 367.4 eV for pure silver is observed. Without annealing, the as-deposited Ag<sub>2</sub>O sample will mainly contain Ag<sub>2</sub>O with a small amount of AgO and Ag grains. According to the current results, the binding energy for 3d<sub>3/2</sub> shifts to a higher value as compared to reported data [21, 22].

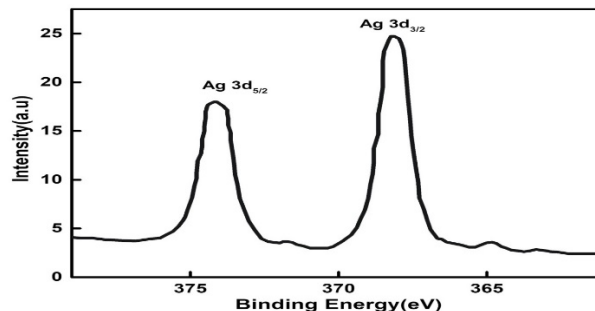


**Fig. 8:** Shows XPS spectra for the sample

## 4. Results and Discussion

Ag<sub>2</sub>O thin films were successfully synthesized on glass substrates using a thermal evaporation technique at room temperature. The focus of the present work is the study of structural and optical properties of Ag<sub>2</sub>O thin films. The structural and morphological studies and microstructural features of silver oxide thin film are determined by using XRD, FESEM, and EDAX. EDAX plot shows particular peaks for silver and oxide and reveals that silver and oxygen are the only elements involved in the synthesis of thin films. In order to find out the optical properties, the films are characterized using laser Raman spectra and UV-visible spectroscopy. Raman spectra at 532 nm give several peaks and the results match with reported literature [13, 14]. XRD plot gives the [h k l] values and gives indices to the different planes and shows the cubic nature of the silver oxide thin film. FESEM gives the microstructural features for different magnifications. FE-SEM results show that the average grain size of silver oxide thin films increased from 38 nm to 43 nm and the average porosity of the film increased from 28 nm to 31 nm. XPS studies were carried out to determine the shift of core level binding energies present in the grown sample, and according to the result observed the binding energy for 3d<sub>3/2</sub> shifts to a higher value.

The standard values for the XPS binding energies of silver and oxygen atoms are 373.8 eV and 367.4 eV, respectively. UV-Vis spectroscopy reveals the films are transparent and absorption edge measures at 380 nm. As a result, a significant violet shift was obtained at the absorption edge

[19]. Thermal evaporation will be used in the future to prepare silver oxide thin film samples doped with Erbium. Furthermore, co-dopants such as Europium will be used to enhance non-linear behavior. These thin films will be investigated for their nonlinear optical properties.

The thin film grown will be used to determine second harmonic generation (if optically possible). The second-order nonlinearity or third-order nonlinearity will be studied and the corresponding  $\chi^{(2)}$  and  $\chi^{(3)}$  will be determined using the Z-scan technique. Mach-Zehnder interferometer will be constructed and devised to find an optical bistable nature. The bistable nature of the thin films will also be studied for eventually finding applications in optical switching, dichroic filters, lasers, etc. It can be further used to characterize the samples for low energy electron diffraction (LEED), neutron diffraction, and electron loss spectroscopy (ELS).

### Acknowledgment

The authors would like to thank TAS (New Delhi) for helping with sample synthesis, as well as Central Instrumentation Laboratory, Guru Jambheshwar University of Science & Technology, Hisar for characterizing the samples. Karamvir thanks CSIR New-Delhi for the JRF/SRF fellowship.

### References

- [1] E. T Salim, M. T. Awayiz, R. O Mahdi, Digest Journal of Nanomaterials and Biostructures **14(4)**, 1151-1159 (2019).
- [2] A. C. Nwanya, Advances in Materials Science and Engineering **1**, 450820 (2013).
- [3] Chiyah, Basma, K. Kayed, International Journal of Nanoelectronics and Materials **11.3**, 305-310 (2018).
- [4] Chouhan, Neelu, Silver nanoparticles. **Vol. 1**, London, UK: Intech Open, (2018).
- [5] Agasti, Souvik, A. Dewasi, A. Mitra, AIP Conference Proceedings **Vol. 1953**, No.1 (2018).
- [6] M. F. Al-Kuhaili, Applied Physics **40(9)**, 2847 (2007).
- [7] E. Fortin, F. L. Weichman, physica status solidi (b) **5(3)**, (1964) 515-519.
- [8] J. F. Pierson, C Rousselot, Surface and Coatings Technology **200(1-4)**, 276-279 (2005).
- [9] Y. C. Her, Y. C. Lan, W. C. Hsu, S. Y Tsai, Journal of Applied Physics, **96(3)**, 1283-1288 (2004).
- [10] A. A. Schmidt, J. Offermann, R. Anton, Thin Solid Films, **281**, 105-107 (1996).
- [11] N. R. C. Raju, K. Jagadeesh Kumar, Journal of Raman Spectroscopy, **42(7)**, 1505-1509 (2011).
- [12] G. Xiao-Yong, F Hong-Liang, M Jiao-Min, Z Zeng-Yuan, Chinese Physics B, **19(9)**, 090701 (2010).
- [13] N. R. C. Raju, K. J. Kumar, A Subrahmanyam, Journal of Physics D: Applied Physics, **42(13)**, 135411 (2009).
- [14] N. T. Tsendzughul, A. A. Ogwu, ACS omega, **4(16)**, 16847-16859 (2019).
- [15] A. Hammad, M. A. Wahab, A. Alshahrie, Dig. J. Nanomater Bios **11.4**, 1245-1252 (2016).
- [16] Mirzaeian, Mojtaba, A: Physicochemical and Engineering Aspects **519**, 223-230 (2017).
- [17] A. I. Oje, Journal of Science: Advanced Materials and Devices **4.2**, 213-222 (2019).
- [18] A. I. Oje, A. A. Ogwu, A. M. Oje, Journal of Electroanalytical Chemistry **882**, 115015 (2021).
- [19] S. Sagadevan, International Journal of Nanoelectronics & Materials, **9(1)**, (2016).
- [20] Y. Chiu, U. Rambabu, M. H. Hsu, H. P. D. Shieh, C. Y. Chen, H. H. Lin, Journal of Applied Physics, **94(3)**, 1996-2001 (2003).
- [21] M. F. Al-Kuhaili, Journal of Physics D: Applied Physics, **40(9)**, 2847(2007).
- [22] R. Snyders, Surface and Coatings Technology **174**, 1282-1286 (2003).

### Biography:



**Karamvir Tanwar** did his B.Sc. (2012) in Non-Medical from Govt. College, Distt. Mahendergarh, Haryana, and completed M.Sc. (2015) in Physics from Guru Jambheshwar University of Science and Technology, Hisar-125001 (Haryana state) - India. Since January 2020, he has been pursuing PhD in the Department of Physics at Guru Jambheshwar University of Science and Technology, Hisar. His Current research includes thin film synthesis and linear and Non-Linear optical physics. He has developed a thermal deposition unit for the synthesis of thin films.



**David Joseph** did his B.Sc. in physics from the University of Kerala (1985) and M.Sc. in physics from Banaras Hindu University, (BHU) in 1988. He consequently did his PhD in the Laser and spectroscopy lab of BHU (1996) on Static laser light scattering. He did his post-doctoral research at the Indian Institute of Technology Kanpur (IITK) in two Laser laboratories. In the period 1997 to 2005, He worked on high-resolution Laser spectroscopy of rare earth-doped crystals at L-He temperatures. From 2005 to 2006, he worked on quantum computing experimental aspects at Femtosecond laser Laboratory at IIT-Kanpur. In 2006 from May to October, he worked on

Laser spectroscopy projects of bio systems as a senior scientist at the Manipal Academy of Higher Education (MAHE), Manipal. In October 2006, he joined the Physics department at Guru Jambheshwar University Hisar, working for the optical Engineering program (M. Tech). He has been working on Non-linear optics, laser spectroscopy, pulsed laser deposition, Static light scattering, and speckle Interferometry and has developed experimental setups for each of them. A Bridgeman– stock- burger crystal growth set-up is also developed through funding from the RUSA grant of DST, Government of India.